Optimization of preparation conditions of a novel low-cost natural bio-sorbent from olive pomace and column adsorption processes on the removal of phenolic compounds from olive oil mill wastewater

Imane HAYDARI
Universite Cadi Ayyad Faculte des Sciences Semlalia
Amina LISSANEDDINE
Universite Cadi Ayyad Faculte des Sciences Semlalia
Khalid AZIZ
Ibn Zohr University Faculty of Science Agadir: Universite Ibn Zohr Faculte des Sciences Agadir
Naaila Ouazzani
Universite Cadi Ayyad Faculte des Sciences Semlalia
Laila MANDI
Universite Cadi Ayyad Faculte des Sciences Semlalia
Ayoub El GHADRAOUI
Universite Cadi Ayyad Faculte des Sciences Semlalia
Faissal Aziz (f.aziz@uca.ma)
Université Cadi Ayyad: Universite Cadi Ayyad https://orcid.org/0000-0001-9144-6400

Research Article

Keywords: Bio-sorbent, Hydrogen peroxide, Olive oil mills wastewater, Olive pomace waste, Phenolic compounds, Regeneration

Posted Date: February 25th, 2022

DOI: https://doi.org/10.21203/rs.3.rs-1314058/v1

Abstract

Olive oil mill wastewater (OMWW) poses an undeniable environmental problem due to its high organic loads and phenolic compounds (PCs) content. This study determined the optimal conditions for preparing a new bio-sorbent from olive pomace (OP) and the adsorptive treatment of OMWW by this bio-sorbent. The activation reaction was performed with hydrogen peroxide. The results of the combination effect optimization of the three preparation variables: the activation temperature (°C) X_1, the activation time (min) X_2 and the impregnation ratio X_3, are presented by the response surface methodology (RSM). The maximum adsorption capacity was obtained at activation time 300 min, temperature 80 °C and ratio equal to 6.2:1. The bio-sorbent was characterized by Fourier transform infrared spectroscopy (FTIR), scanning electron microscopy (SEM), energy-dispersive X-ray spectroscopy (EDS) and X-ray diffractometer (XRD). The adsorption process performance of this bio-sorbent was examined in batch and fixed-bed columns. An adsorption capacity of 446 mg g^{-1} has been achieved for 4000 mg L^{-1} concentration of PCs. The adsorption isotherm and kinetics were consistent with the Langmuir and pseudo-second-order models. Therefore, the Thomas model best fit the fixed bed column experimental data. The bio-sorbent gave a high desorption percentage of PCs, which was above 70% using HCl (0.1M).

Introduction

The cultivation of the olive tree is part of the Mediterranean tradition. It is a symbol of civilization among the Mediterranean peoples and, at the same time, a favorite dish of their table. In addition to its main product, oil leaves two by-products: the OP and the vegetation water, also called OMWW. However, these effluents have a low economic value in Morocco (Lissaneddine et al. 2021).

OMWW is viscous, acidic and rich in organic matter (total sugars, nitrogenous substances, organic acids, PCs, fats) (Achak et al. 2009; Lissaneddine et al. 2021). Therefore, the OMWW poses an undeniable environmental problem because of their high chemical oxygen demand (COD) content and the presence of PCs. Since these PCs cause inhibition of seed germination and plant growth (Elayadi et al. 2019). Consequently, also affect groundwater, surface water, and soil (Dhouib et al. 2006). However, these PCs have economic value if recovered, as they are characterized by a high antioxidant activity (Aissa et al. 2017). In addition, those PCs are considered as additives for numerous consumable products (Ciriminna et al. 2017) and cosmetic uses (Galanakis et al. 2018). Therefore, the main appeal in PCs offers an opportunity for high-added-value by-products that may reimburse the treatment expense of the OMWW and give a considerable edge for earnings.

Different techniques for PCs removing from OMWW have been studied (adsorption, coagulation-flocculation, artificial wetlands, distillation, infiltration-percolation and distillation) (Achak et al. 2009; Leone et al. 2017; Elayadi et al. 2019; Papaoikonomou et al. 2019). But these processes show several limitations, such as being more expensive, generating large amounts of sludge and incomplete removal of pollutants. However, researchers have focused on the adsorption technique, which is considered the

cheapest, simple and most effective method for removing and recovering different types of pollutants (Boumya et al. 2021; Lissaneddine et al. 2021).

For large scale applications, it's mandatory to carry out continuous flow treatment using a column model to evaluate the intended contact time in which the adsorbate attain an equilibrium (Aziz et al. 2020). Fixed-bed processes have advantages such as ease of operation, high efficiency, lowest cost, large wastewater flows can be treated by an adequate amount of porous material, and the possibility of regeneration (Aksu and Gönen 2004; Lakshmipathy and Sarada 2015; Aziz et al. 2020).

In similar recent works, they studied the activation of olive pomace (OP) by CuO (Yuney et al. 2020), NaOH (Lissaneddine et al. 2021) and KOH (Şirazi and Aslan 2021) to adsorb PCs from OMWW. However, those works performed a carbonization step at an elevated temperature during the adsorbent preparation. Moreover, this adsorbent was only tested under batch conditions on diluted OMWW. These reasons make their adsorbent difficult to prepare, and it isn't easy to apply in the industry. Therefore, it is suggested in the present study to use raw OMWW and bio-sorbents activated with hydrogen peroxide only in an activation step without carbonization.

The objective of the present work was to prepare a bio-sorbent from OP and then employ it as a low-cost adsorbent for the recovery of PCs from OMWW, which represent a green circular economy approach. First, MINITAB software was used to determine the optimal conditions for the preparation of the bio-sorbent. Then, batch adsorption experiments were performed under different operational conditions (contact time, initial solution pH, initial PCs concentration and temperature). Finally, a fixed bed reactor was used to remove and regenerate the bio-sorbent, targeting a large-scale application.

Materials And Methods

1. Sample collection and characterization physic-chemical of OMWW

The OMWW samples were collected in the region of Marrakech-Safı of Morocco during the 2020/2021 olive oil extraction season.

Measurements of pH and electrical conductivity are performed by a probe Hanna HI 9829. The chemical oxygen demand (COD) was estimated by oxidation with an excess of potassium dichromate in a hot and acidic environment according to the standard (AFNOR T 90-101). The Kjeldahl nitrogen, Nitrite, Nitrates, Orthophosphate, Total phosphorus and Sulfate are determined according to the standards AFNOR T90-110, AFNOR T90-013, RODIER 1984, AFNOR T90-022, AFNOR T90-023 and RODIER 7th EDITION, respectively. The concentration PCs were determined by the Folin-Ciocalteu method (Singleton and Rossi, 1965) using caffeic acid as the standard.

2. Preparation of bio-sorbent

In this study, we used an OP waste was located in the region of Marrakech-Safi, Morocco. After washing with distilled water, the OP was dried in an oven at 105°C (SF7/S Stuart, United Kingdom) for 24 hours. Hydrogen peroxide H_2O_2 is a chemical agent used to produce a bio-sorbent with chemical activation. OP samples were mixed by stirring with 250 g of hydrogen peroxide H_2O_2 solution (10%) at different temperatures under stirring. The resulting bio-sorbent was washed with distilled water and dried in an oven at 60°C for 24 hours.

3. Characterization of bio-sorbent

The physicochemical characteristics of the bio-sorbent were studied using XRD. FTIR (ALPHA-P, Germany) was used to characterize the functional groups in the wavelength range of 400–4000 cm^{-1}. In addition, pore size distribution, specific surface area and pore volume were evaluated by N_2 sorption measurements using Brunauer Emmett and Teller S_{BET}. Examination of the grain morphology of the bio-sorbent was performed using SEM measurements (Fuveau, France), which were taken with a scanning microscope, The analysis of elements on the micro-scale and element distribution on the bio-sorbent by EDS analyzer (TEAM™ EDS).

4. Experimental setup and procedure

4.1. Batch adsorption and isotherm studies

The bio-sorbent prepared was studied as an adsorbent for the adsorption of PCs from OMWW. The effect of contact time on the adsorption process of PCs was evaluated in the range of 0 - 240 min at optimum values of adsorbent dose 25 mg, initial concentration 4000 mg L^{-1}, at pH 4.0 and temperature 25°C with a stirring speed of 200 rpm (KS 3000i control, Germany). Concerning the study of the PCs concentration effect on the adsorption capacity, a series of concentrations was carried out 2000, 3000 and 4000 mg L^{-1}, for 240 min and at pH 4.0. This corresponds to the effect of pH; OMWW was adjusted to values ranging from 2.0 to 12.0 by adding hydrochloric acid (HCl) or sodium hydroxide (NaOH) of equal concentrations to 1.0N. To study the effect of temperature, the adsorption process was performed at temperatures of 20, 40 and 60°C. In an adsorbent dose of 25 mg, a volume of 25 mL of OMWW, at a concentration of 4000 mg L^{-1} and pH 4.0.

The adsorption capacity was determined according to equation (eq. (1)):

$$q = \frac{(C_0 - C_t)}{W} * V \quad \text{(Eq. 1)}$$

Where, C_t (mg L^{-1}) is the PCs concentration after a certain time of contact with bio-sorbent, C_o (mg L^{-1}) is the initial concentration of PCs, V is the volume of solution (L) and W is the amount of bio-sorbent (g).

4.1.1. Langmuir model

Langmuir model is based on several assumptions and adsorption is limited to monolayer adsorption. The energy of adsorption is assumed to be the same all over the surface; no interactions between adjacent

molecules on the surface and molecules adsorb at fixed sites and do not migrate over the surface as given by the equation (eq. (2)). As a result, the Langmuir isotherm equation has the following by Okeola and Odebunmi (2010) and Aliakbarian et al. (2015):

$$\frac{C_e}{q_e} = \frac{1}{K_l * q_m} + \frac{C_e}{q_m} \text{(Eq. 2)}$$

Where, q_e (mg g^{-1}) is the amount of PCs adsorbed at equilibrium; C_e (g L^{-1}) is the concentration of PCs at equilibrium; K_L is the Langmuir constant related to the energy of adsorption (L g^{-1}); and q_m (mg g^{-1}) is the maximum adsorption capacity.

4.1.2. Freundlich model

The Freundlich isotherm mainly describes the adsorption equilibrium of sorption on a heterogeneous surface and is given by the equations (eq. (3)). The Freundlich isotherm equation is expressed by Okeola and Odebunmi (2010) and Aliakbarian et al. (2015):

$$logq_e = \log K_F + \left(\frac{1}{n}\right)\log C_e \text{(Eq. 3)}$$

Where, n is the adsorption intensity constant, K_F is the Freundlich constant indicating adsorption capacity.

4.2. Column adsorption and isotherm studies

The experiment column adsorption was conducted using a tube with a height of 30 cm and a diameter of 0.5 cm. The bio-sorbent dose 4.5 g was introduced into the column. The OMWW was introduced in ascending flow using a pump (Antlia - 3C Dutscher, France) at a constant flow rate of 0.5 mL min^{-1}. All experiments are carried out at a temperature of 60°C for 120 min, with samples taken every 15 min.

4.2.1. Thomas model

The Thomas model (Thomas, 1944) is based on the assumption that the adsorption is of the Langmuir type; the adsorption kinetics obey reversible second order kinetics. This model applies to a system with a constant flow rate and without axial dispersion. This model is given by equation (eq. (4)) (Aksu and Gönen 2004):

$$\frac{C}{C_0} = \frac{1}{(1 + exp?\,(K_{Th} * q_{Th} * \frac{m}{Q} - K_{Th} * C_0 * t)} \text{ (Eq. 4)}$$

Where, k_{TH} (mL min^{-1} mg^{-1}) is the Thomas rate constant; q_0 (mg g^{-1}) is the adsorption capacity; m total amount of bio-sorbent sent to the column (g); and Q is the flow rate that circulates through the column (mL min^{-1}).

4.2.2. Yoon-Nelson model

The Yoon and Nelson model (Yoon and Nelson 1984) assumes that the decrease in adsorption probability for each adsorbate molecule is proportional to the solute adsorption probability and the adsorbate breakthrough probability (Gong et al. 2015). The Yoon-Nelson equation is written as follows:

$$\frac{C}{C_0} = \frac{exp?\,(K_{YN} * t - * K_{YN})}{1 + exp?\,(K_{YN} * t - * K_{YN})} \text{(Eq. 5)}$$

Where, k_{YN} the Yoon-Nelson rate constant (min^{-1}) and τ is the time required for 5 % adsorbate breakthrough (min).

5. Desorption

Desorption gives the bio-sorbent a chance for reuse. The desorption tests were done in the same way as the adsorption experiments. First, the bio-sorbent was saturated with PCs and then washed with distilled water in the first series. Next, desorption of the bio-sorbent was done with 0.1M HCl solution at 60°C. Then, the bio-sorbent is reused for further PCs adsorption tests. Finally, the desorbed amount of PCs was calculated by equation (eq. (6)).

Desorbed = $\frac{q_r}{q_0} * 100\%$ (Eq. 6)

Where, q_r and q_0 (mg g^{-1}) are adsorption capacities of the PCs after and before regeneration, respectively.

6. Statistical analysis

The effect of process parameters on the optimal bio-sorbent preparation conditions and adsorption capacity was analyzed using the MINITAB statistical software.

The MINITAB software is a statistical technique used to identify significant parameters to determine the optimal bio-sorbent preparation conditions. The three parameters chosen for the experiment were the activation temperature X1, activation time X2 and rate X3 rate. Each parameter has three different levels (coded as -1, 0 and +1): Activation temperature (60, 70 and 80°C), activation time (180, 240 and 300 min), and rate (3.1:1, 4.6:1 and 6.2:1) (Table 1). The three parameters studied yielded twelve experimental designs.

Modeling of the optimal bio-sorbent preparation conditions was based on the second-order polynomial equation (eq. (7)):

$$y = b0 + \sum_{i=1}^{n} bixi + \sum_{i=1}^{n} biix^2 i + \sum_{i=j}^{n-1} \sum_{j=i+1}^{n} bijxij \quad \text{(Eq. 7)}$$

Where, b_0 the constant, bi the linear effect of input factor x_i, b_{ij} the linear by a linear interaction effect between input factors x_i, x_j, b_{ij} the quadratic effect of input factor x_i, n number of factors.

In addition, the statistical software MINITAB was used to study the effect of operating conditions on the adsorption capacity. Finally, an analysis of variance was performed to determine the significance of the interactions and effects between the operating conditions.

Table 1
Actual and coded values of independent variables used for Minitab

Process variables	Units	Symbols	Levels		
			-1	0	1
Activation time	Min	X1	180	240	300
Activation temperature	°C	X2	60	70	80
Ratio		X3	3.1:1	4.6:1	6.2:1

Results And Discussion

1. Phys-chemical properties of the OMWW

The physicochemical analysis of the studied OMWW (Table 2) shows these effluents have an acidic pH (4.81), indicating that OMWW is an acidic effluent. The same pH value was observed by Bouknana et al. (2014), Lee et al. (2019), Dehmani et al. (2020) and Lissaneddine et al. (2021). Table 2 shows a lower electrical conductivity (12 mS cm^{-1}) than that found by Lissaneddine et al. (2021), Elayadi et al. (2021) and El Ghadraoui et al. (2021). The Chemical Oxygen Demand (80 g O_2. L^{-1}) is high and is also characterized by a predominance of toxic substances and the presence of PCs (Vuppala et al. 2021). Inorganic loadings such as potassium (4.8 g L^{-1}), and sodium (0.3 g L^{-1}).

Table 2
Physicochemical parameters of the OMWW

Parameters (Unit)	OMWW
pH	4.81
Electrical Conductivity (mS cm^{-1})	12
COD (g-O_2 L^{-1})	84.1
Total phosphorus (mg L^{-1})	2.54
Orthophosphate (mg L^{-1})	1.69
Nitrite (mg L^{-1})	0.06
Sodium (g L^{-1})	0.3
Potassium (g L^{-1})	4.8
Ammoniacal nitrogen (mg L^{-1})	0.96
Kjeldahl nitrogen (NTK) (mg L^{-1})	215
Sulfate (mg L^{-1})	2769.23
Nitrate (mg L^{-1})	0.331

2. Characterization of the bio-sorbent

Figure 1(a and b) shows the FTIR spectrum of OP before and after treatment by hydrogen peroxide. FTIR spectrums were obtained in the wavelength range of 480-4000 cm^{-1}. The FTIR spectrum of OP waste (Fig. 1a), the peak at 3457 cm^{-1}, can be attributed to the -OH stretching vibration. The peak at 2925 cm^{-1} is due to C-H stretching vibrations in aliphatic CH, CH_2, and CH_3. The peaks at 1461 and 1645 cm^{-1} were attributed to the symmetrical stretching vibrations of CH_2 and C=O groups, respectively (Wang et al. 2019). The FTIR spectrum of bio-sorbent (Fig. 2b) at 3416 cm^{-1} corresponds to the -OH of hydroxyl functional groups. The peak at 1628 cm^{-1} is attributed to the stretching vibration of carboxylic groups -C=O (Martín-Lara et al. 2008), the bond at 1380 cm^{-1} is attributed to the symmetrical stretching vibration CH_2 (Allwar et al. 2020). The peak at 1033 cm^{-1} can be attributed to the bending vibration of the -OH group (Nasrullah et al. 2018). The FTIR spectra (Fig. 2c) between the bio-sorbent before and after PCs adsorption showed no significant difference.

Biosorption can be explained by the interaction between the functional groups present on the bio-sorbent and the CPs, considering two types of chemical and physical interactions. Biosorption involves different mechanisms such as coordination, complexation, microprecipitation or electrostatic attraction (Veglio

and Beolchini 1994). Identifying these processes and the characterization of the active sites of the bio-sorbent are essential steps for optimizing the operating conditions in the development of the adsorption capacity of PCs.

SEM analysis allows visualization of the bio-sorbent pores. This analysis was performed to determine the elements present on the surface of the samples by EDX. The results obtained from olive pomace before and after chemical activation at the same magnifications are presented in Fig. 2.

Figure 2a shows that the surface of the olive pomace does not contain pores or voids. However, after activation, relatively more homogeneous pores with constant diameters appeared on the external surface of the bio-sorbent, improving the porosity; consequently, a high number of pores on the surface of the bio-sorbent.

The EDX analysis of the OP before and after activation allowed the elemental analysis of the elements present on the external surface. The analysis shows that both materials are composed mainly of carbon atoms and contain oxygen (Table 3a). After activation (Table 3b), Mg and Cu appear on the surface.

Şirazi et al. (2021) observed similar texture characteristics using OP activated by KOH. This shows that the OP's SEM surface before activation has a porosity less than that of the adsorbent after activation, which is similar to the present study results.

Table 3 EDX spectra of OP before (a) and after chemical activation (b)

(a)

Element	Atomic %
C	74.13
O	24.46
Si	0.26
P	0.26
S	0.17
K	0.54
Ca	0.18
Total	100

(b)

Element	Atomic %
C	70.50
O	29.10
Cu	0.22
Mg	0.18
Totals	100

The XRD patterns for pure and activated OP are shown in Fig. 3. The XRD patterns of OP before and after activation are very similar, suggesting that no alteration of the OP structure occurred during the preparation of the bio-sorbent. This is normal because we only did a chemical activation without carbonization. The two diffractograms showed peaks located at 2θ = 22.31° (Trache et al. 2014), 39.16°, 45.43°, 61.58°, 77.65°, 84. 47°, which is attributed to the native cellulose, while the other constituents of OP are mainly amorphous, which is explained by the appearance of the spectrum Schneider and Brenbner (1985) and Zhang et al. (2015).

The pH at which the zero surface charge is called the point of zero charges (pzc). The surface's electrokinetic properties are defined by pH_{PZC} (Yagub et al. 2014). The plot $pH_f = f(pH_i)$ is shown in Fig. 4. Results show that pH_{PZC} of the bio-sorbent was around 8.64.

This value, superior to 7, indicates a concordance between this result, the acid's contents, and the surface's basic functions. Thus, the bio-sorbent surface is positively charged for pH values lower than pH_{PZC}. As a result, the solution will become less acidic (consumption of protons from the solution), while for higher values, the surface is negatively charged, and the solution will become more acidic (release of surface protons). This is consistent with the result obtained by Şirazi et al. (2021) since the KOH-activated OP, pH_{PZC} for adsorbent, was 8.0.

3. Process optimization

3.1. Optimization of preparation conditions for bio-sorbent

The preparation variables are presented in a design matrix; their ranges and responses (adsorption capacity (mg g^{-1})) are displayed in Table 4. The statistical software MINITAB is applied to compare and correlate the independent variables in Table 5. It was applied to develop polynomial regression equations, representing all quadratic expressions suggested by MINITAB. The equation expression was selected according to the sequential sum of the square model, which is based on the highest order of the polynomial where the model was not aliased and the extra terms were significant (Sahu et al. 2010; Garba et al. 2014; Salman 2014). There was a clear correlation between the experimental and predicted

data, as indicated by the model R^2 values 0.9745 for adsorption capacity. The final empirical model equation for the Yq response of the adsorption capacity is given by equation (eq. (8)):

$Y_q = 686 - 3.72X_1 - 13.9X_2 + 85X_3 + 0.00583X_1^2 + 0.190X_2^2 + 58.3X_3^2 + 0.0292X_1X_2 + 0.238X_1X_3 - 2.98X_2X_3$ (Eq. 8)

Table 4
Minitab experimental design

Run	Level			Variables			Repones
				X_1	X_2	X_3	q (mg g^{-1})
1	-1	-1	-1	240	60	3.1: 1	273.21
2	+1	+1	-1	180	60	4.6: 1	123.21
3	-1	-1	-1	240	60	6.2: 1	326.78
4	+1	+1	-1	180	80	4.6: 1	416.35
5	-1	-1	+1	180	70	3.1: 1	340.71
6	+1	+1	+1	240	80	6.2: 1	486.07
7	-1	-1	+1	180	70	6.2: 1	305.35
8	+1	+1	+1	300	60	4.6: 1	292.85
9	-1.682	0	0	240	80	3.1: 1	551.78
10	+1.682	0	0	300	70	6.2: 1	510.71
11	0	-1.682	0	240	70	4.6: 1	332.14
12	0	+1.682	0	240	70	4.6: 1	332.14
13	0	0	-1.682	300	70	3.1: 1	489.00
14	0	0	+1.682	240	70	4.6: 1	332.14
15	0	0	0	300	80	4.6: 1	656.00

Table 5
Regression analysis (ANOVA) for response surface methodology

Source	df	Sum of Squares	Mean Square	F-Value	p-Value
Model	9	242316	26924	21.20	0.002
A-Time	1	72758	72758	57.28	0.001
B-Temperature	1	149644	149644	117.81	0.000
C-Ratio	1	83	83	0.07	0.808
A^2	1	1624	1624	1.28	0.309
B^2	1	1332	1332	1.05	0.353
C^2	1	12563	12563	9.89	0.026
AB	1	1225	1225	0.96	0.371
AC	1	814	814	0.64	0.460
BC	1	3557	3557	2.80	0.155

Table 4 represents the variance (ANOVA) results of the full factional design using the statistical software MINITAB. The model F-value was recorded at 21.20, enlightening that the model was significant. On the other hand, high values of R^2 (0.9745) and Adj-R^2 (0.9285) were estimated, indicating that the selected model can describe 92.85% of the total variation on adsorption capacity data. The parameters having a p-value probability value of less than 0.05 are significant. In this case, A, B and C^2 are the significant model terms. Values superior to 0.1 are considered non-significant terms.

3.2. The Pareto chart

The presentation of the relative importance of the main effects and their interaction was achieved using the Pareto chart, as shown in Fig. 5. The individual factors and the likely combinations obtained are represented as bars. To show whether the effects studied differ significantly from zero, the t-test was used (Abdel-ghani et al. 2016). For a 97.45% confidence level and nine degrees of freedom, the t-test value was found to be equal to 2.57. The values on the horizontal axes are the t-test values for each effect and their interaction (Carmona et al. 2005; Rathinam et al. 2011; Saadat and Karimi-Jashni 2011). Variables A, B and C^2 have an absolute value greater than 2.57, which places them on the right side of the vertical line and makes them significant. While all other factors have an absolute value below the reference line, making them insignificant. By analyzing the Pareto chart, it can be seen that B, A and C^2 have the greatest influence on the adsorption of PCs in the bio-sorbent. On the other hand, the effect of ratio (C) made the smallest contribution to the adsorption of PCs into bio-sorbent because it is far from the reference line of the Pareto chart.

3.3. Contour plots and response surface

The 3D contour plots and response surface show the interactive effects of several parameters on the response. The contour plots and response surface were acquired by Minitab software to indicate the adsorption efficiency of PCs considering independent factors such as activation time, activation temperature and ratio were shown in Fig. 6. The effect of activation time, ratio and activation temperature was investigated using response surface methodology (RSM) by Minitab software. From Table 5, the F-value of the model is 21.20 and the p-value is 0.023. The model terms were considered significant when the p-value was less than 0.05. The contour plot (Fig. 6a) for the interaction between activation time and ratio shows at time 300 min and ratio 6.2:1 (3) the interaction was declared significant. The graph of the interaction between activation temperature and ratio (Fig. 6b) shows that at ratio 3.2:1(1) and temperature 80°C, the adsorption of PCs is significant. The interaction between activation temperature and activation time (Fig. 6c) indicates at time 300 min and temperature 80°C, the biosorption is significant.

The optimal conditions for bio-sorbent preparation using response optimization were obtained at ratio = 6.2:1 (3), activation time = 300 min and activation temperature = 80°C.

4. Adsorption efficiency

4.1. Batch adsorption

4.1.1. Effect of initial concentration

The driving force is very important by the initial concentration of PCs to overcome all the mass transfer limitations between the two phases, liquid and solid (Liu et al. 2019).

The plot of adsorption capacity versus time at different concentrations was presented in Fig. 7. The maximum adsorption capacity is 789.28 mg g^{-1}, at the initial phenol concentration of 4000 mg L^{-1} and time 120 min. This increase in adsorption capacity with increasing concentration was attributed to the fact that this concentration was the driving force in order to overcome the resistance in the mass transfer of PCs between the liquid phase (OMWW) and the solid phase (bio-sorbent surface), resulting in the increase of their transfer rate into the adsorbent (Lissaneddine et al. 2021). Comparing the results with different studies, the adsorption of PCs on activated carbon by Achak et al. (2009) reported a decrease in adsorption efficiency with an increase in the initial concentration. This phenomenon was attributed to activated carbon adsorbing more phenolic compounds at low initial concentrations than higher initial concentrations. On the other hand, in the study of Lissaneddine et al. (2021) on the use of SA-AC beads for the adsorption of PCs, an increase in adsorption capacity was observed with the increase in initial

concentration. This is due to the increasing amount of PCs in the solution, which causes a rise in the mass transfer driving force (Liu et al. 2019).

4.1.2. Adsorption isotherm

When the adsorption process reached equilibrium, the adsorption isotherms were analyzed to describe the distribution of PCs between the solid and liquid phases (Liu et al. 2019). Several models have been proposed to describe this relationship during the adsorption of PCs OMWW, the main ones being the isothermal models of Langmuir and Freundlich. Some assumptions are applicable according to the Langmuir theory. First of all, all sites are energetically equivalent, i.e., the energy of the adsorption sites is considered equal, while they can contain at most one adsorbate molecule, forming a monolayer on the adsorbent surface. In addition, the surface of the adsorbent is assumed to be homogeneous, with the identification of the active sites. Moreover, there is no interaction between the adsorbed molecules (Swenson and Stadie 2019). On the contrary, Freundlich's theory considers the heterogeneous adsorption surface, while several layers of adsorbate molecules can be formed. Furthermore, this theory considers that interactions between adsorbed molecules occur (Dada et al. 2012; Osagie and Owabor 2015). Figure 8 shows the adsorption isotherm of PCs with the bio-sorbent. The adsorption capacity of PCs increased with the increase of PCs concentration until it reached 789.28 mg g^{-1} at the concentration of 4000 mg L^{-1}. The driving force of mass transfer is the increase of the PCs concentration in the solution (Li et al. 2019).

From the linear regression data (Table 6) in Fig. 9(a and b), it is clear that the model with a correlation coefficient (R^2= 0.9898), indicating that the active adsorption sites of PCs on the bio-sorbent are energetically homogeneous and a significant monolayer coverage of PCs on the outer surface of the bio-sorbent is formed without any interaction between the PCs (Mojoudi et al. 2019). Therefore, the Langmuir model represents the best model for the adsorption of PCs onto the bio-sorbent with a maximum adsorption capacity is 1125 mg g^{-1}.

Table 6
Parameters of adsorption isotherms of PCs on bio-sorbent

Freundlich			**Langmuir**		
K_F (mg $^{1-(1/n)}$ $L^{1/n}$ g^{-1})	n	R^2	K_L (L mg^{-1})	q_m (mg g^{-1})	R^2
0.934	1.22	0.967	16.10^{-3}	1250	0.9898

4.1.3. Effect of contact time

The effect of contact time allowed the essential parameters during adsorption. Adsorption time can vary depending on the nature of adsorbent and adsorbate, while it is affected by different parameters, such as

concentration of PCs in the solution, temperature, and pH of the OMWW. In all cases, the equilibrium is reached at a given time; this is the state in which the increase of the contact time does not significantly increase PC adsorption efficiency. The equilibrium time varies with the studied adsorbents, such as SA-AC beads (120 min) (Lissaneddine et al. 2021), pomegranate seed (20 min) (Papaoikonomou et al. 2019), the raw clay (10 min) (Chaari et al. 2020), $MgCl_2$-impregnated activated carbons (60 min) (Hamadneh et al. 2020) and hydroxyapatite-sodium alginate composite (Benaddi et al. 2021).

Figure 10 shows the sorption equilibrium obtained after about 150 min, then remains stable with an adsorption capacity value of 789.28 mg g^{-1}. Adsorption can be considered a two-step process, a rapid initial adsorption step, attributed to many adsorption sites available on the bio-sorbent for PCs adsorption. This rapid step leads to a rapid increase in the amount of PCs accumulated on the bio-sorbent surface. Existing residual sites are then difficult to occupy by PCs, as repulsive forces develop between the PCs on the solid surface of the bio-sorbent and the bulk phase (Lissaneddine et al. 2021). In addition, PCs are small molecules and can diffuse into the internal pores (Papaoikonomou et al. 2019), thus reducing the driving force for mass transfer (Din et al. 2009). Obviously, during the slow step, the molecules encounter greater resistance to enter the adsorption sites (Lissaneddine et al. 2021; Achak et al. 2009).

4.1.4. Adsorption kinetic

The adsorption kinetic study provides important information to predict the adsorption process. In this work, two linear kinetic models studied the adsorption of PCs from OMWW by the bio-sorbent as a function of time, including pseudo-first-order and pseudo-second-order.

From Fig. 11, both models show clear linearity of the equation with a correlation value of R^2=0.9456 for pseudo-first-order kinetics and a correlation of R^2=0.992 for pseudo-second-order kinetics. Therefore, according to Table 7, the model with the experimentally calculated maximum equilibrium sorption capacity value approximately equal to that determined theoretically is the pseudo-first-order. Therefore, the adsorption kinetics of PCs on the bio-sorbent is of pseudo-second-order type. Furthermore, this model assumes that the sorption of PCs is mainly controlled by chemisorption, which includes valence changes through electron exchange or partitioning between the bio-sorbent and PCs. Therefore, external adsorption occurs more often than micropore adsorption (Abdelhay et al. 2017; Tao et al. 2019).

In a batch test, the bio-sorbent removed 789.28 mg g^{-1} of PCs. Compared to olive pomace treated with H_3PO^{4+} $2MHNO_3$ (28.57 mg g^{-1}) (Soudani et al. 2013), HCl + $ZnCl_2$ (78.74 mg g^{-1}) (Temdrara et al. 2015) and H_3PO_4 (110.30 mg g^{-1}) (Soudani et al. 2017). The bio-sorbent of this study showed better removal efficiency of PCs.

Table 7
Values of characteristics constants for two models of adsorption kinetic

Pseudo-first-order				Pseudo-second-order			
q_{ethero} (mg g^{-1})	q_{eexp} (mg g^{-1})	K_{lag} (min^{-1})	R^2	q_{ethero} (mg g^{-1})	q_{eexp} (mg g^{-1})	K_b (mg g^{-1} min^{-1})	R^2
446	408.92	0.024	0.9456	446	423.21	60.64×10^{-4}	0.9929

4.1.5. Effect pH

pH is a more important parameter in the adsorption process. The pH affects the sorption mechanisms onto the bio-sorbent surface and the nature of physicochemical interactions between the bio-sorbent adsorption sites and the PCs (Achak et al. 2009). In addition, pH can also affect the surface charge of the adsorbent (Aksu and Gönen 2004).

The adsorption capacity as a function of time at different pH values was shown in Fig. 12. A significant effect of pH on the adsorption of PCs was observed. It can be explained by the π-π electron donor-acceptor interactions between the aromatic ring of the PCs (electron acceptor) and the free oxygen of the surface basic sites (electron donor) (Moreno-Castilla 2004; Dabrowski et al. 2005; Hamdaoui and Naffrechoux 2007). The adsorption capacity of PCs on the bio-sorbent increases from 150 to 473 mg g^{-1} for pH values between 2 and 4, the maximum adsorption of PCs is reached at pH equal to 4.0. If the pH value is exceeded 4.0, there is a decrease in the adsorption capacity of PCs. This decrease can be attributed to the phenol ionization to phenolate ions form since the absorption of this later is prevented by hydroxyl ions presented on the adsorbent (Halhouli and Darwish 1995). The adsorption capacity is higher at acidic pH than at basic pH. The pH of the OMWW is acidic, which is advantageous in this study, so pH adjustment would not be necessary during effluent treatment. Therefore, OMWW can be used directly without pH adjustment in large-scale treatment systems, which minimizes costs during treatment. A study by Alwan (2008) showed that pH adjustment in industrial wastewater treatment plants influences the treatment efficiency, which leads to an increase in wastewater treatment cost.

4.1.6. Effect of temperature

Temperature is one of the most important parameters during the sorption process. Figure 13 shows the plot of adsorption capacity versus time at different temperatures. The maximum adsorption capacity is found to be 1307 mg g^{-1} at a temperature of 60°C. The increase in adsorption capacity with increasing temperature can be attributed to the increase in temperature promoting the polymerization phenomenon between the PCs, increasing adsorption efficiency. Furthermore, this increase in adsorption capacity can be associated with an increase in adsorbent swelling, allowing more active sites of the bio-sorbent to

become available to the adsorbate (Ververi and Goula 2019). However, the temperature is a parameter that depends on other characteristics of the adsorbent and the solution (Moreno-Castilla 2004).

4.1.7. Thermodynamic studies

The thermodynamic parameters (ΔG^0), (ΔH^0) and (ΔS^0) were calculated by using the following equations 10 and 11:

$$\Delta G^\circ = \Delta H^\circ - T \times \Delta S^\circ \text{(Eq. 10)}$$

$$lnK_c = -\frac{\Delta H^\circ}{R \times T} + \frac{\Delta S^\circ}{R} \text{(Eq. 11)}$$

Plotting ln(*Kc*) as a function of 1/T (Fig. 14) allows the calculated ΔH^0, ΔG^0 and ΔS^0. The thermodynamic parameters for the adsorption of PCs onto the bio-sorbent are given in Table 8. The value of ΔG^0 for all three temperatures was obtained negative, confirming the spontaneous and feasible adsorption of PCs on the bio-sorbent. In addition, the ΔG^0 values for physisorption are less than -20 kJ mol^{-1} and chemisorption is greater than -80 kJ mol^{-1} (Turco et al. 2019). In this work, ΔG^0 was -4229.38, -4355.49, -4732.51 and -5036.33 J $mol^{-1,}$ which indicated the adsorption of PCs with the bio-sorbent is chemisorption. In addition, ΔH^0 and ΔS^0 are other critical thermodynamic parameters that provide information about the adsorption process of PCs. In this study, the positive value of ΔH^0 was 30.82 kJ mol^{-1}, which demonstrates the endothermic nature of the adsorption process of PCs with the bio-sorbent. As for ΔS^0, a positive value was obtained 49.26 J mol^{-1} K^{-1}, so the increased randomness can explain it at the liquid/solid interface during the adsorption process (Sun et al. 2005). These outcomes are identical to those of Lissaneddine et al. (2021), who have found that $\Delta S° = 74$ J K^{-1} mol^{-1} and $\Delta H° = 29$ kJ mol^{-1}.

Table 8
Thermodynamic parameters of adsorption of PCs onto bio-sorbent

ΔG^0 (J mol^{-1})				ΔH^0 (KJ mol^{-1})	ΔS^0 (J mol^{-1} K^{-1})
293.5K	298.5K	313.5K	333.5K		
-4229.38	-4355.49	-4732.51	-5036.33	30.82	49.26

5. Fixed-bed column

A continuous fixed-bed column adsorption process using a bio-sorbent as a sorbent was considered an alternative method to separate PCs from OMWW. Figure 15 shows the breakthrough curves for the adsorption of PCs on bio-sorbent in a fixed-bed column adsorption system at 60°C.

In Fig. 15, C_0 is the initial concentration of PCs entering the column and C_t is the concentration of PCs leaving the column every 15 minutes. All PCs were adsorbed in the first 40 minutes, resulting in a low concentration of PCs in OMWW output. During the adsorption process, the concentration of PCs in the treated effluent gradually increases. The bio-sorbent sites are saturated and the adsorption zone progresses vertically in the column (Kundu and Gupta, 2005). In our work, the q_e value reached 643.92 mg g^{-1} for C_i= 4251 mg L^{-1} and Q= 0.5 mL min^{-1}, while the removal rate was 64% (Table 9).

Using Yoon-Nelson and Thomas's empirical models, the mathematical analysis of PCs adsorption study data on fixed-bed columns were analyzed. The model proposed by Yoon-Nelson considers the adsorption probability of each molecule to be directly proportional to the breakthrough probability of the adsorbate on the adsorbent and the adsorption probability of the adsorbate (Ajmani et al. 2020). The Thomas model is a theoretical model commonly applied in analyzing column adsorption data. It is based on the assumptions of the Langmuir isotherm model and the second-order kinetic model of the batch adsorption process (Ajmani et al. 2020). The Yoon-Nelson and Thomas model parameters for the PCs adsorption on the bio-sorbent in a fixed-bed column are presented in Table 10.

From Table 10, the Yoon-Nelson model correlates R^2= 0.9572, demonstrating that the Yoon-Nelson model was approachable and could be used to describe the adsorption of PCs in continuous mode on the bio-sorbent. Table 10 shows that the mean absolute error (MAE) values were 0.0125 and 0.0104 for the Yoon-Nelson and Thomas model, respectively. In contrast, the two models' root means square error (RMSE) values were calculated as 0.12 and 0.10, respectively. The RMSE and MAE values of the Thomas model were lower than those of the Yoon-Nelson model. The Thomas model fit the experimental data; the results followed Langmuir kinetics (Chue 2010).

Table 9
Parameters of breakthrough curves of the packed bed column for PCs adsorption onto the bio-sorbent

C_i (mg L^{-1})	Q (mL min^{-1})	V_{ef} (mL)	m_{total} (mg)	R (%)	q_e (mg g^{-1})
4251	0.5	60	500	64	643.92

Table 10
Parameters of Thomas and Yoon-Nelson model for the adsorption of PCs into bio-sorbent in a fixed-bed column

Model	Parameters	Value
Thomas	K_{Th} (mL mg^{-1} min^{-1})	0.00144
	$q_{0\ cal}$ (mg g^{-1})	547.78
	R^2	0.94571
	MAE	0.0104
	RMSE	0.10
Yoon-Nelson	K_{YN} (min^{-1})	0.3411
	t_{Cal} (min)	57
	R^2	0.9571
	MAE	0.0125
	RMSE	0.12

6. Desorption

The desorption study aims to elucidate the adsorption process, the recovery of PCs, and the adsorbents' reuse. In the first adsorption cycle, the bio-sorbent was saturated with PCs with a removal rate of 64%. Then, the bio-sorbent was washed with distilled water and treated with 0.1M HCl solution for 120 min at room temperature. The adsorption process was duplicated several times, and the efficiency of the bio-sorbent in removing PCs was analyzed. At the second reuse cycle, the adsorption rate of the bio-sorbent is decreased from 64 to 30% (Fig. 16), which shows that the bio-sorbent is a good sorbent with excellent reusability and stability. Several studies on the desorption of PCs for adsorbent regeneration have been performed. According to Lissaneddine et al. (2021), who used Sodium-alginate-active carbon beads, the percentage of desorption of PCs was 58.5%. Yuney et al. (2020) used CuO-coated OP, reaching 77% of the PCs concentration desorbed.

Conclusion

In this paper, we are interested in testing the effectiveness of new bio-sorbent low-cost in removing PCs from OMWW in a continuous flow. The optimum condition of preparation of the bio-sorbent was determined using the statistical software MINITAB. The structure of bio-sorbent was characterized by FTIR and Brunauer, Emmett and teller S_{BET}. The adsorption of PCs was found to be dependent on the

contact time, initial concentration, pH solution and temperature. The Langmuir isotherm best represented the equilibrium adsorption data, and the adsorption capacity was found to be 446 mg g^{-1}. The adsorption kinetics was described well by the pseudo-second-order model. The positive ΔH° value demonstrated that the adsorption was endothermic, and the negative ΔG° indicated the spontaneous adsorption reaction. Thomas is the best model that was better at predicting PCs column adsorption. The yield desorption decreases from 74 to 36% in the two cycles. To conclude, bio-sorbent can be stated among the effective alternatives for PC sorption since it provides ready separation and easy recycling from low-cost solutions.

Declarations

Acknowledgements

This work was supported by the Morocco-Tunisian bilateral scientific cooperation project (20 /PRD-MT-02).

Competing interest: The authors declare that they have no known competing financial interests or personal relationships that could have influenced the work reported in this paper.

Ethics approval and consent to participate: We all declare that manuscript reporting studies do not involve any human participants, human data, or human tissue. So it is not applicable.

Consent for publication: Our manuscript does not contain data from any individual person, so it is “Not applicable.”

Data availability and materials: The datasets and materials used and/or analyzed during the current study are available from the corresponding author on reasonable request.

Funding information: This work was supported by the Morocco-Tunisian bilateral scientific cooperation project (20 /PRD-MT-02).

Authors’ Contributions: Imane HAYDARI (Data curation) (writing - original draft), (interpretation). **Amina LISSANEDDINE** (optimization) (Review and editing). **Khalid AZIZ** (Modelization) (Review and editing). **Naaila OUAZZANI** (Review and editing). **Laila MANDI** (Review and editing). **Ayoub El GHADRAOUI** (Participating in Data curation). **Faissal AZIZ** (Supervision) (Review and editing).

References

1. Abdel-Ghani NT, El-Chaghaby GA, Elgammal MH, Rawash ESA (2016) Optimizing the preparation conditions of activated carbons from olive cake using KOH activation. https://doi.org/10.1016/S1872-5805(16)60027-6. Xinxing Tan Cailiao/New Carbon Materials

2. Abdelhay A, al Bsoul A, Al-Othman A, Al-Ananzeh NM, Jum'h I, Al-Taani AA (2018) Kinetic and thermodynamic study of phosphate removal from water by adsorption onto (Arundo donax) reeds. Adsorpt Sci Technol. https://doi.org/10.1177/0263617416684347
3. Achak M, Hafidi A, Ouazzani N, Sayadi S, Mandi L (2009) Low cost biosorbent "banana peel" for the removal of phenolic compounds from olive mill wastewater: Kinetic and equilibrium studies. J Hazard Mater. https://doi.org/10.1016/j.jhazmat.2008.11.036
4. Aissa I, Kharrat N, Aloui F, Sellami M, Bouaziz M, Gargouri Y (2017) Valorization of antioxidants extracted from olive mill wastewater. Biotechnol Appl Chem. https://doi.org/10.1002/bab.1509
5. Ajmani A, Patra C, Subbiah S, Narayanasamy S (2020) Packed bed column studies of hexavalent chromium adsorption by zinc chloride activated carbon synthesized from Phanera vahlii fruit biomass. J Environ Chem Eng. https://doi.org/10.1016/j.jece.2020.103825
6. Aksu Z, Gönen F (2004) Biosorption of phenol by immobilized activated sludge in a continuous packed bed: Prediction of breakthrough curves. Process Biochem 8. https://doi.org/10.1016/S0032-9592(03)00132
7. Aliakbarian B, Casazza AA, Perego P (2015) Kinetic and isotherm modelling of the adsorption of phenolic compounds from olive mill wastewater onto activated carbon. Food Technol Biotechnol. https://doi.org/10.17113/ftb.53.02.15.3790
8. Alslaibi TM, Abustan I, Ahmad MA, Foul AA (2014) Kinetics and equilibrium adsorption of iron (II), lead (II), and copper (II) onto activated carbon prepared from olive stone waste. Desalination Water Treat. https://doi.org/10.1080/19443994.2013.833875
9. Alslaibi TM, Abustan I, Ahmad MA, Foul AA (2013) Cadmium removal from aqueous solution using microwaved olive stone activated carbon. J Environ Chem Eng. https://doi.org/10.1016/j.jece.2013.06.028
10. Alwan GM (2008) PH Control Problems of a Wastewater Treatment Plant. Al-Khwarizmi Engineering Journal. https://www.researchgate.net/publication/320191097
11. April Allwar A (2020) Preparation and characterizations of activated carbon from banana fruit bunch with chemical treatments using hydrothermal processes. AIP Conference Proceedings. AIP Publishing. https://doi.org/10.1063/5.0002794
12. Aziz F, Achaby M, Lissaneddine A, Aziz K, Ouazzani N, Mamouni R, Mandi L (2020) Composites with alginate beads: A novel design of nano-adsorbents impregnation for large-scale continuous flow wastewater treatment pilots. Saudi J Biol Sci. https://doi.org/10.1016/j.sjbs.2019.11.019
13. Basu M, Guha AK, Ray L (2019) Adsorption of Lead on Lentil Husk in Fixed Bed Column Bioreactor. Bioresour Technol. https://doi.org/10.1016/j.biortech.2019.02.133
14. Benaddi R, Aziz F, Harfi K, El, Ouazzani N (2021) Adsorption and desorption studies of phenolic compounds on hydroxyapatite-sodium alginate composite. Desalination Water Treat. https://doi.org/10.5004/dwt.2021.26979
15. Bouknana D, Hammouti B, Salghi R, Jodeh S, Zarrouk A (2014) Physicochemical Characterization of Olive Oil Mill Wastewaters in the eastern region of Morocco. J Mater Environ Sci.

http://dx.doi.org/10.22159/jcr.2018v5i5.28840

16. Boumya W, Taoufik N, Achak M, Barka N (2021) Chemically modified carbon-based electrodes for the determination of paracetamol in drugs and biological samples. J Pharm Anal. https://doi.org/10.1016/j.jpha.2020.11.003
17. Cañizares P, Carmona M, Baraza O, Delgado A, Rodrigo MA (2006) Adsorption equilibrium of phenol onto chemically modified activated carbon F400. J Hazard Mater. https://doi.org/10.1016/j.jhazmat.2005.09.037
18. Carmona MER, da Silva MAP, Ferreira Leite SG (2005) Biosorption of chromium using factorial experimental design. Process Biochem. https://doi.org/10.1016/j.procbio.2004.02.024
19. Chaari I, Touil A, Medhioub M (2020) Adsorption-desorption of phenolic compounds from Olive mills wastewater using Tunisian natural clay. Chin J Chem Eng. https://doi.org/10.1016/j.cjche.2020.12.020
20. Chue KH (2010) Fixed bed sorption: Setting the record straight on the Bohart-Adams and Thomas models. J Hazard Mater. https://doi.org/10.1016/j.jhazmat.2010.01.019
21. Ciriminna R, Meneguzzo F, Delisi R, Pagliaro M (2017) Olive Biophenols as New Antioxidant Additives in Food and Beverage. ChemistrySelect. https://doi.org/10.1002/slct.201601900
22. Dabrowski A, Podkościelny P, Hubicki Z, Barczak M (2005) Adsorption of phenolic compounds by activated carbon - A critical review. Chemosphere 58:1049–1070. https://doi.org/10.1016/j.chemosphere.2004.09.067
23. Dada A, Olalekan A, Olatunya A, Dada O (2012) Langmuir, Freundlich, Temkin and Dubinin–Radushkevich isotherms studies of equilibrium sorption of Zn2+ unto phosphoric acid modified rice husk. IOSR J Appl Chem. https://doi.org/10.9790/5736-0313845
24. Dehmani Y, Ed-dra A, Zennouhi O, Bouymajane A, Rhazi F, Nassiri L, Abouarnadasse S (2020) Heliyon Chemical characterization and adsorption of oil mill wastewater on Moroccan clay in order to be used in the agricultural fi eld. https://doi.org/10.1016/j.heliyon.2020.e03164. Heliyon
25. Dermeche S, Nadour M, Larroche C, Moulti-Mati F, Michaud P (2013) Olive mill wastes: Biochemical characterizations and valorization strategies. In Process Biochemistry. https://doi.org/10.1016/j.procbio.2013.07.010
26. Dhouib A, Aloui F, Hamad N, Sayadi S (2006) Pilot-plant treatment of olive mill wastewaters by Phanerochaete chrysosporium coupled to anaerobic digestion and ultrafiltration. https://doi.org/10.1016/j.procbio.2005.06.008
27. Din ATM, Hameed BH, Ahmad AL (2009) Batch adsorption of phenol onto physiochemical-activated coconut shell. https://doi.org/10.1016/j.jhazmat.2008.05.009
28. El Ghadraoui A, Ouazzani N, Saf C, Ahmali A, Hejjaj A, Aziz F, Del Bubba M, Mandi L (2021) Behaviour of physicochemical and microbiological characteristics of vertical flow constructed wetland substrate after treating a mixture of urban and olive mill wastewaters. Environ Sci Pollut Res. https://doi.org/10.1007/s11356-021-14874-7

29. Elayadi F, Achak M, Beniich N, Belaqziz M, El Adlouni C (2020) Factorial design for optimizing and modeling the removal of organic pollutants from olive mill wastewater using a novel low-cost bioadsorbent. Water Air Soil Pollut. https://doi.org/10.1007/s11270-020-04695-8
30. Elmansour TE, Mandi L, Ahmali A, Elghadraoui A, Aziz F, Hejjaj A, del Bubba M, Ouazzani N (2020) Effect of polyphenols on activated sludge biomass during the treatment of highly diluted olive mill wastewaters: biomass dynamics and purifying performances. Water Sci Technol. https://doi.org/10.2166/wst.2020.423
31. Ena A, Pintucci C, Carlozzi P (2012) The recovery of polyphenols from olive mill waste using two adsorbing vegetable matrices. J Biotechnol. https://doi.org/10.1016/j.jbiotec.2011.06.027
32. Galanakis CM, Tsatalas P, Galanakis IM (2018) Implementation of phenols recovered from olive mill wastewater as UV booster in cosmetics. Ind Crops Prod. https://doi.org/10.1016/j.indcrop.2017.09.058
33. Garba ZN, Rahim AA (2015) Optimization of activated carbon preparation conditions from Prosopis africana seed hulls for the removal of 2,4,6-Trichlorophenol from aqueous solution. Desalination Water Treat. https://doi.org/10.1080/19443994.2014.963150
34. Gong JL, Zhang YL, Jiang Y, Zeng GM, Cui ZH, Liu K, Deng CH, Niu QY, Deng JH, Huan SY (2015) Continuous adsorption of Pb(II) and methylene blue by engineered graphite oxide coated sand in fixed-bed column. Appl Surf Sci. https://doi.org/10.1016/j.apsusc.2014.11.068
35. Halhouli KA, Darwish NA, Al NM (1995) Separation Science and Technology Effects of pH and Inorganic Salts on the Adsorption of Phenol from Aqueous Systems on Activated Decolorizing Charcoal. Sep Sci Technol. https://doi.org/10.1080/01496399508013147
36. Hamdaoui O, Naffrechoux E (2007) Modeling of adsorption isotherms of phenol and chlorophenols onto granular activated carbon Part I Two-parameter models and equations allowing determination of thermodynamic parameters. J Hazard Mater. https://doi.org/10.1016/j.jhazmat.2007.01.021
37. Kilic MY, Abdelraheem WH, He X, Kestioglu K, Dionysiou DD (2019) Photochemical treatment of tyrosol, a model phenolic compound present in olive mill wastewater, by hydroxyl and sulfate radical-based advanced oxidation processes (AOPs). J Hazard Mater. https://doi.org/10.1016/j.jhazmat.2018.06.062
38. Kundu S, Gupta AK (2005) Analysis and modeling of fixed bed column operations on As(V) removal by adsorption onto iron oxide-coated cement (IOCC). J Colloid Interface Sci. https://doi.org/10.1016/j.jcis.2005.04.006
39. Lakshmipathy R, Sarada NC (2015) A fixed bed column study for the removal of Pb2+ ions by watermelon rind. Environ Sci Water Res Technol. https://doi.org/10.1039/c4ew00027g
40. Leone L, Almeida D, Aguiar Á, Teixeira C, Francisco A, Magliano F, Amaro V, Duarte L, Filho V, Wanderley-teixeira V (2017) exposed to sub-lethal doses of herbicides. Acta Histochem. https://doi.org/10.1016/j.acthis.2017.01.003
41. Lin SH, Juang RS (2009) Adsorption of phenol and its derivatives from water using synthetic resins and low-cost natural adsorbents: A review. J Environ Manage 90:1336–1349.

https://doi.org/10.1016/j.jenvman.2008.09.003

42. Lissaneddine A, Mandi L, El M, Mousset E, Rene ER, Ouazzani N, Aziz F (2021) Chemosphere Performance and dynamic modeling of a continuously operated pomace olive packed bed for olive mill wastewater treatment and phenol recovery. https://doi.org/10.1016/j.chemosphere.2021.130797
43. Liu QS, Zheng T, Wang P, Jiang JP, Li N (2010) Adsorption isotherm, kinetic and mechanism studies of some substituted phenols on activated carbon fibers. Chem Eng J. https://doi.org/10.1016/j.cej.2009.11.013
44. Liu X, Xu J, Zhao Y, Shi H, Huang CH (2019) Hydrophobic sorption behaviors of 17B-Estradiol on environmental microplastics. Chemosphere. https://doi.org/10.1016/j.chemosphere.2019.03.162
45. Martín-Lara MA, Pagnanelli F, Mainelli S, Calero M, Toro L (2008) Chemical treatment of olive pomace: Effect on acid-basic properties and metal biosorption capacity. J Hazard Mater. https://doi.org/10.1016/j.jhazmat.2007.12.035
46. Mojoudi N, Soleimani M, Mirghaffari N, Belver C, Bedia J (2019) Removal of phenol and phosphate from aqueous solutions using activated carbons prepared from oily sludge through physical and chemical activation. Water Sci Technol. https://doi.org/10.2166/wst.2019.305
47. Mondal NK, Samanta A, Dutta S, Chattoraj S (2017) Optimization of Cr(VI) biosorption onto Aspergillus niger using 3-level Box-Behnken design: Equilibrium, kinetic, thermodynamic and regeneration studies. J Genetic Eng Biotechnol. https://doi.org/10.1016/j.jgeb.2017.01.006
48. Moreno-Castilla C (2004) Adsorption of organic molecules from aqueous solutions on carbon materials. Carbon. https://doi.org/10.1016/j.carbon.2003.09.022
49. Nasrullah A, Bhat AH, Naeem A, Isa MH, Danish M (2018) High surface area mesoporous activated carbon-alginate beads for efficient removal of methylene blue. Int J Biol Macromol. https://doi.org/10.1016/j.ijbiomac.2017.10.045
50. Okeola FO, Odebunmi EO (2010) Freundlich and Langmuir isotherms parameters for adsorption of methylene blue by activated carbon derived from Agrowastes. Advances in Natural and Applied Sciences. https://link.gale.com/apps/doc/A252944801/AONE?u=anon~ec2f229c&sid=googleScholar&xid=b01749a5
51. Osagie E, Owabor CN (2015) Adsorption of Benzene in Batch System in Natural Clay and Sandy Soil. Adv Chem Eng Sci. https://doi.org/10.4236/aces.2015.53037
52. Papaoikonomou L, Labanaris K, Kaderides K, Goula AM (2019) Adsorption – desorption of phenolic compounds from olive mill wastewater using a novel low-cost biosorbent. Environ Sci Pollut Res Int. https://doi.org/10.1007/s11356-019-07277-2
53. Paraskeva P, Diamadopoulos E (2006) Technologies for olive mill wastewater (OMW) treatment: A review. J Chem Technol Biotechnol 81:1475–1485. https://doi.org/10.1002/jctb.1553
54. Patel H (2019) Fixed-bed column adsorption study: a comprehensive review. Appl Water Sci 9:45. https://doi.org/10.1007/s13201-019-0927-7
55. Imad Hamadneh RA, Abu-Zurayk AH, Al-Dujaili (2020) Removal of phenolic compounds from aqueous solution using MgCl 2-impregnated activated carbons derived from olive husk: the effect of

chemical structures. Water Sci Technol. https://doi.org/10.2166/wst.2020.297

56. Rathinam A, Rao JR, Nair BU (2011) Adsorption of phenol onto activated carbon from seaweed: Determination of the optimal experimental parameters using factorial design. J Taiwan Inst Chem Eng. https://doi.org/10.1016/j.jtice.2011.04.003
57. Rodis PS, Karathanos VT, Mantzavinou A (2002) Partitioning of olive oil antioxidants between oil and water phases. J Agric Food Chem. https://doi.org/10.1021/jf010864j
58. Saadat S, Karimi-Jashni A (2011) Optimization of Pb(II) adsorption onto modified walnut shells using factorial design and simplex methodologies. Chem Eng J. https://doi.org/10.1016/j.cej.2011.08.042
59. Sabah H, Thouraya T, Melek H, Nadia M (2020) Application of Response Surface Methodology for Optimization of Cadmium Ion Removal from an Aqueous Solution by Eggshell Powder. Chem Res Chin Univ. https://doi.org/10.1007/s40242-015-7163-9
60. Sadaf S, Bhatti HN (2014) Batch and fixed bed column studies for the removal of Indosol Yellow BG dye by peanut husk. J Taiwan Inst Chem Eng. https://doi.org/10.1016/j.jtice.2013.05.004
61. Sahu JN, Acharya J, Meikap BC (2010) Optimization of production conditions for activated carbons from Tamarind wood by zinc chloride using response surface methodology. Bioresour Technol. https://doi.org/10.1016/j.biortech.2009.10.031
62. Salman JM (2014) Optimization of preparation conditions for activated carbon from palm oil fronds using response surface methodology on removal of pesticides from aqueous solution. Arab J Chem. https://doi.org/10.1016/j.arabjc.2013.05.033
63. Schneider MH, Brebner KI (1985) Wood-polymer combinations: The chemical modification of wood by alkoxysilane coupling agents. Wood Sci Technol. https://doi.org/10.1007/BF00354754
64. Singleton VL, Rossi JA (1965) Colorimetry of total phenolics with phosphomolybdic-phosphotungstic acid reagents.American Journal of Enology and Viticulture. http://www.ajevonline.org/content/16/3/144.full.pdf+html
65. Şirazi M, Aslan S (2021) Comprehensive characterization of high surface area activated carbon prepared from olive pomace by KOH activation. Chem Eng Commun. https://doi.org/10.1080/00986445.2020.1864628
66. Soudani N, Najar-Souissi S, Abderkader-Fernandez VK, Ouederni A (2017) Effects of nitrogen plasma treatment on the surface characteristics of olive stone-based activated carbon. Environ Technol. https://doi.org/10.1080/09593330.2016.1214626
67. Soudani N, Souissi-Najar S, Ouederni A (2013) Influence of nitric acid concentration on characteristics of olive stone based activated carbon. Chin J Chem Eng. https://doi.org/10.1016/S1004-9541(13)60638-2
68. Swenson H, Stadie NP (2019) Langmuir ' s Theory of Adsorption: a. Centennial Rev 35:5409–5426. https://doi.org/10.1021/acs.langmuir.9b00154
69. Sun J, Liu X, Zhang F, Zhou J, Wu J, Alsaedi A, Hayat T, Li J (2019) Insight into the mechanism of adsorption of phenol and resorcinol on activated carbons with different oxidation degrees. Colloids

and Surfaces A Physicochemical and Engineering Aspects. https://doi.org/10.1016/j.colsurfa.2018.11.042

70. Tao J, Huo P, Fu Z, Zhang J, Yang Z, Zhang D (2019) Characterization and phenol adsorption performance of activated carbon prepared from tea residue by NaOH activation. Environ Technol. https://doi.org/10.1080/09593330.2017.1384069
71. Temdrara L, Addoun A, Khelifi A (2015) Development of olivestones-activated carbons by physical, chemical and physicochemical methods for phenol removal: a comparative study. Desalination Water Treat. https://doi.org/10.1080/19443994.2013.838523
72. Thomas HC (1944) Heterogeneous Ion Exchange in a Flowing System. J Am Chem Soc. https://doi.org/10.1021/ja01238a017
73. Trache D, Donnot A, Khimeche K, Benelmir R, Brosse N (2014) Physico-chemical properties and thermal stability of microcrystalline cellulose isolated from Alfa fibres. Carbohydr Polym. https://doi.org/10.1016/j.carbpol.2014.01.058
74. Turco A, Pennetta A, Caroli A, Mazzotta E, Monteduro AG, Primiceri E, de Benedetto G, Malitesta C (2019) Easy fabrication of mussel inspired coated foam and its optimization for the facile removal of copper from aqueous solutions. J Colloid Interface Sci. https://doi.org/10.1016/j.jcis.2019.05.059
75. Veglio F, Beolchini F (1997) Removal of metals by biosorption: a review. Hydrometallurgy 44:301–316. https://doi.org/10.1016/S0304-386X(96)00059-X
76. Ververi M, Goula AM (2019) Pomegranate peel and orange juice by- product as new biosorbents ofphenolic compounds from olive mill wastewaters. Chem Eng Process 138:86–96. https://doi.org/10. 1016/j.cep.2019.03.010
77. Vuppala S, Shaik RU (2021) applied sciences Multi-Response Optimization of Coagulation and Flocculation of Olive Mill Wastewater: Statistical Approach. Appl Sci https://doi.org/10.3390/app11052344
78. Wang W, Xu S, Wang K, Liang J, Zhang W (2019) De-intercalation of the intercalated potassium in the preparation of activated carbons by KOH activation. Fuel Processing Technology. https://doi.org/10.1016/j.fuproc.2019.03.001
79. Yagub MT, Sen TK, Afroze S, Ang HM (2014) Dye and its removal from aqueous solution by adsorption: A review. Adv Colloid Interface Sci 209:172–184. https://doi.org/10.1016/j.cis.2014.04.002
80. Yoon YH, Nelson JH (1984) Application of Gas Adsorption Kinetics I. A Theoretical Model for Respirator Cartridge Service Life. https://doi.org/10.1080/15298668491400197. American Industrial Hygiene Association Journal
81. Yuney K, Oladipo AA, Gazi M, Younis DZ (2020) Chemosphere CuO coated olive cake nanocomposites for rapid phenol removal and effective discoloration of high strength olive mill wastewater. Chemosphere. https://doi.org/10.1016/j.chemosphere.2020.126703
82. Zhang F, Pang Z, Dong C, Liu Z (2015) Preparing cationic cotton linter cellulose with high substitution degree by ultrasonic treatment. Carbohydr Polym.

https://doi.org/10.1016/j.carbpol.2015.06.055

Figures

Figure 1

FTIR spectra of olive pomace waste (a), bio-sorbent before (b) and after (c) adsorption of the PCs

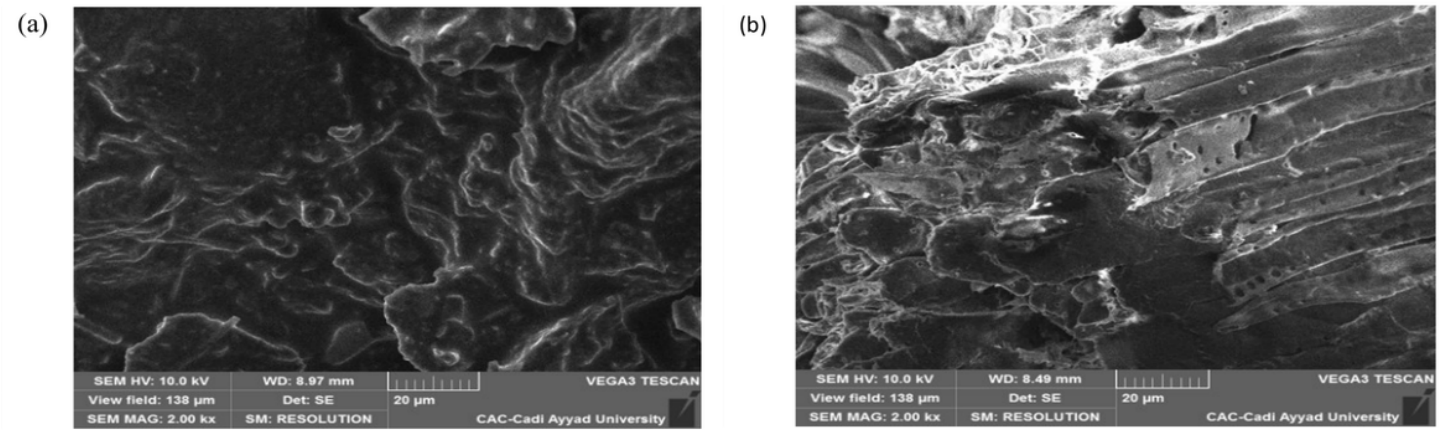

Figure 2

SEM of OP waste before (a) and after chemical activation (b)

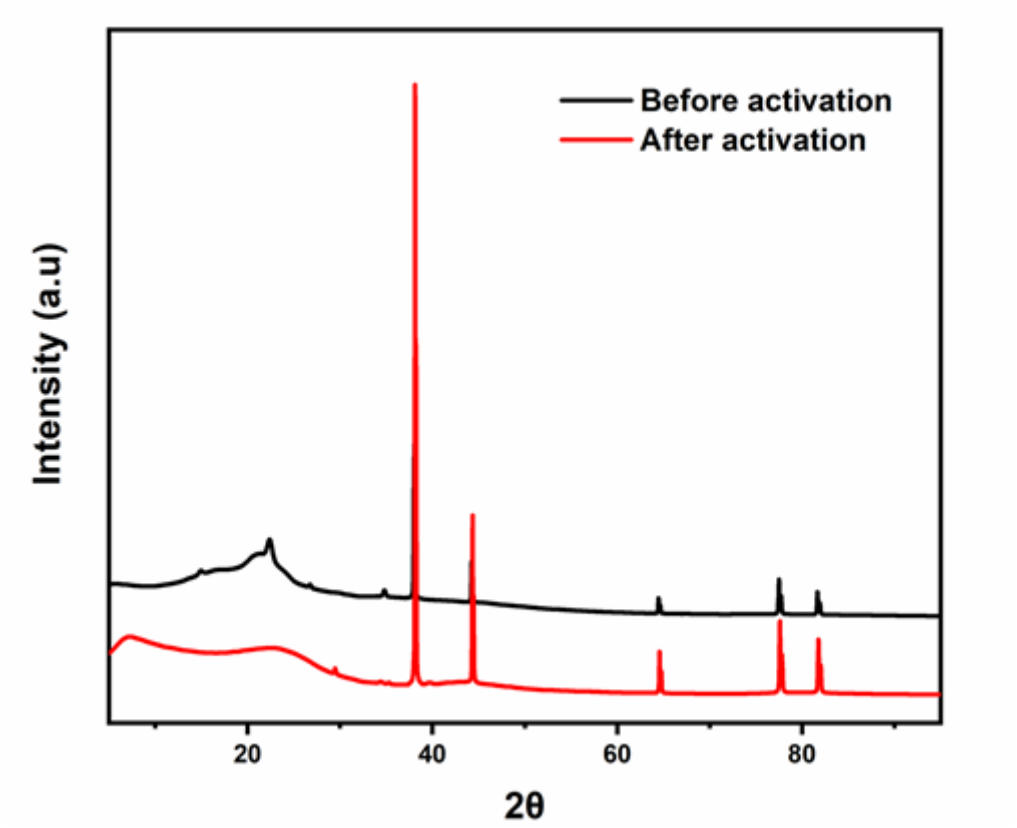

Figure 3

XRD of OP before and after activation

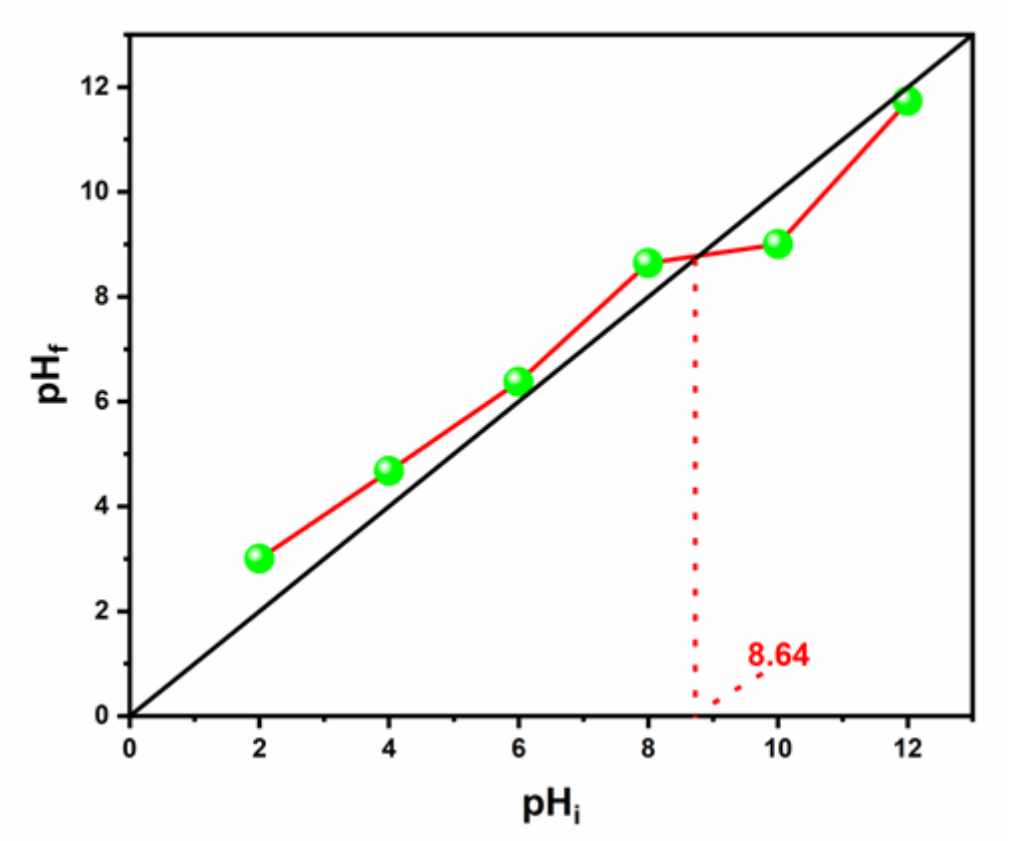

Figure 4

pH_{ZPC} of bio-sorbent

Figure 5

Pareto chart indicating the significant parameters

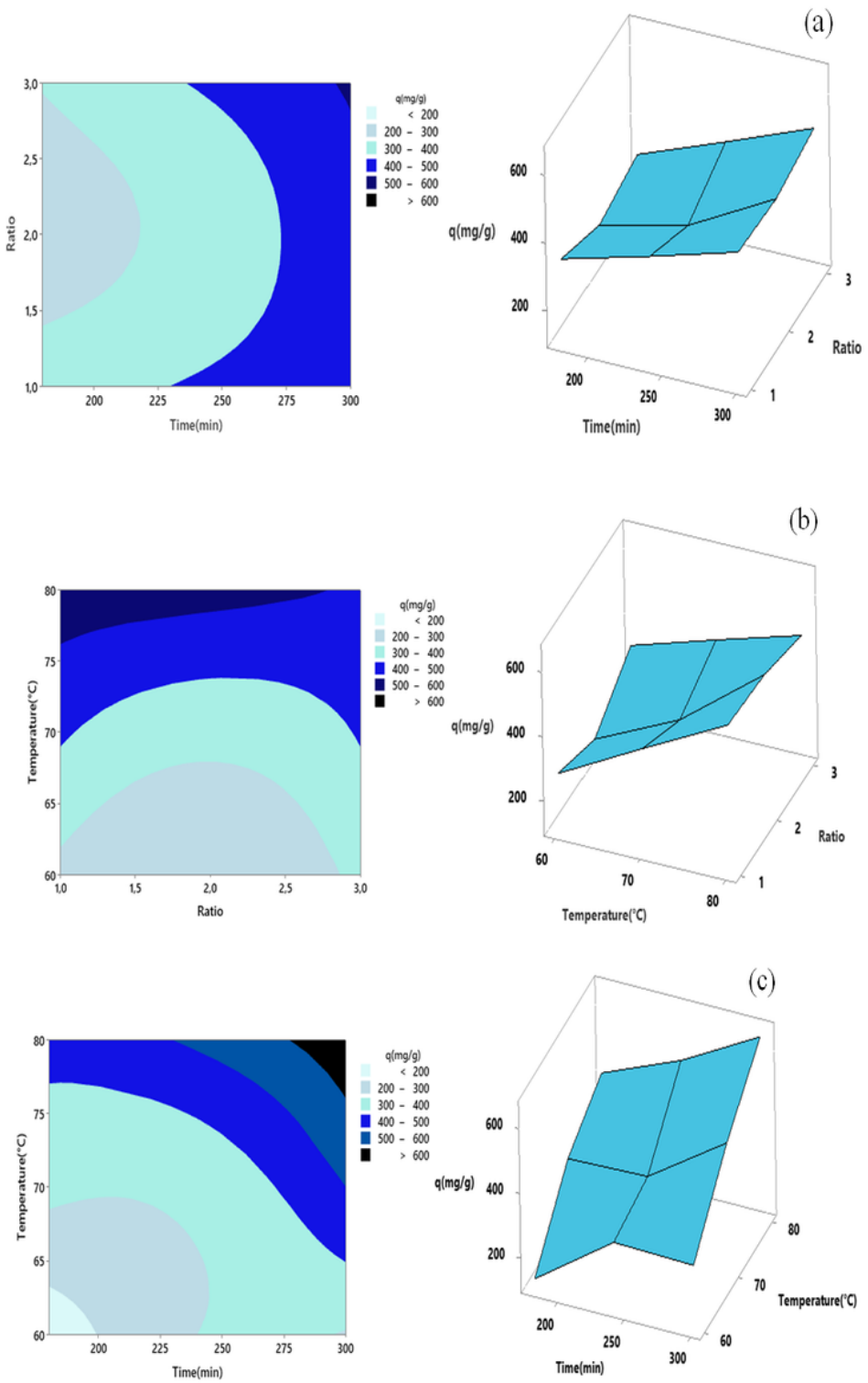

Figure 6

The representative contour plots and 3D-response surface of effect for the interaction between the activation time (min) and ratio (a), activation temperature (°C) and ratio (b) and the activation time (min) and activation temperature (°C) and ratio (c) on capacity adsorption (mg g^{-1})

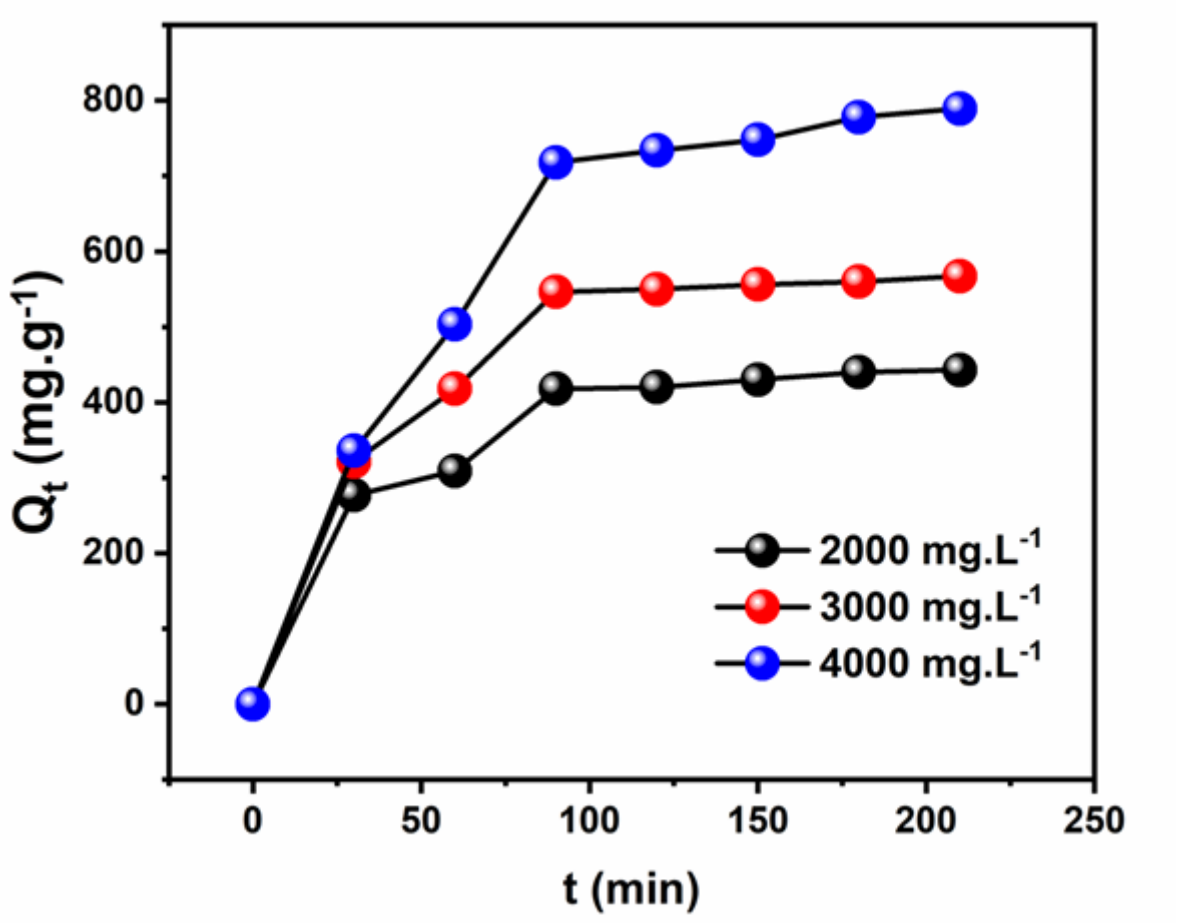

Figure 7

Efect of initial concentration (PCs, 2000–4000 mg L^{-1}; volume of OMWW, 25 mL; temperature, 20 °C; pH = 4.0; and contact time, 240 min)

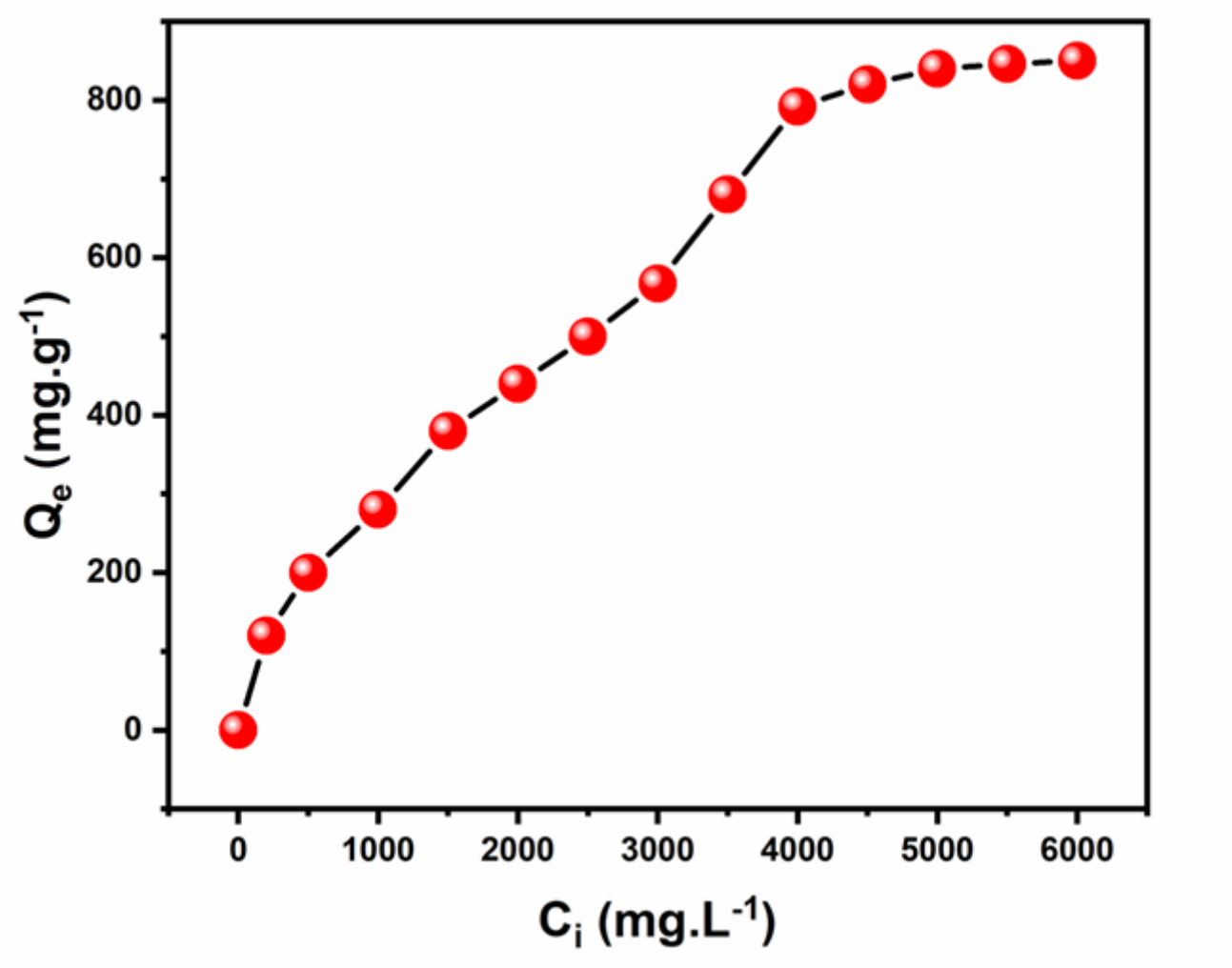

Figure 8

Efect of initial concentration (PCs, 2000–4000 mg L^{-1}; volume of OMWW, 25 mL; temperature, 20 °C; pH = 4.0; and contact time, 240 min)

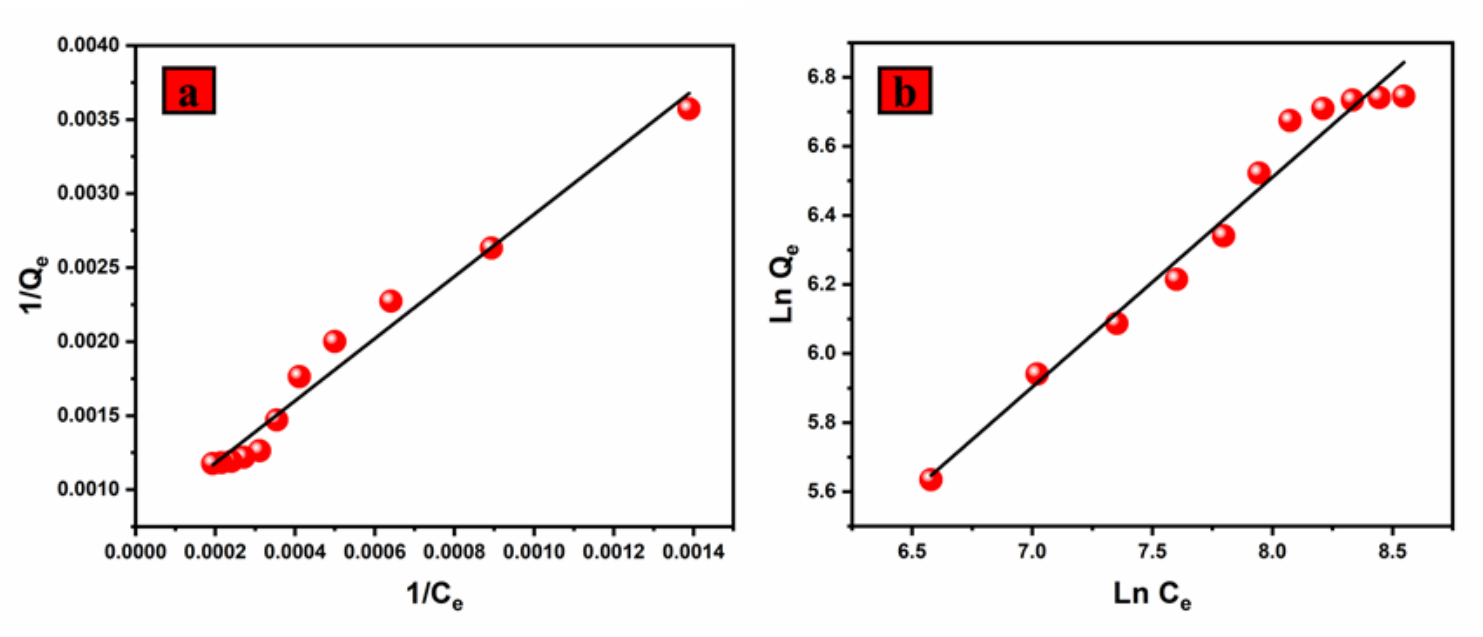

Figure 9

Modeling of the adsorption isotherm of PCs by Langmuir (a) and Freundlich (b) model (Temperature, 20 °C; volume of OMWW, 25 ml; rot =200 rpm; time, 210 min; pH= 4)

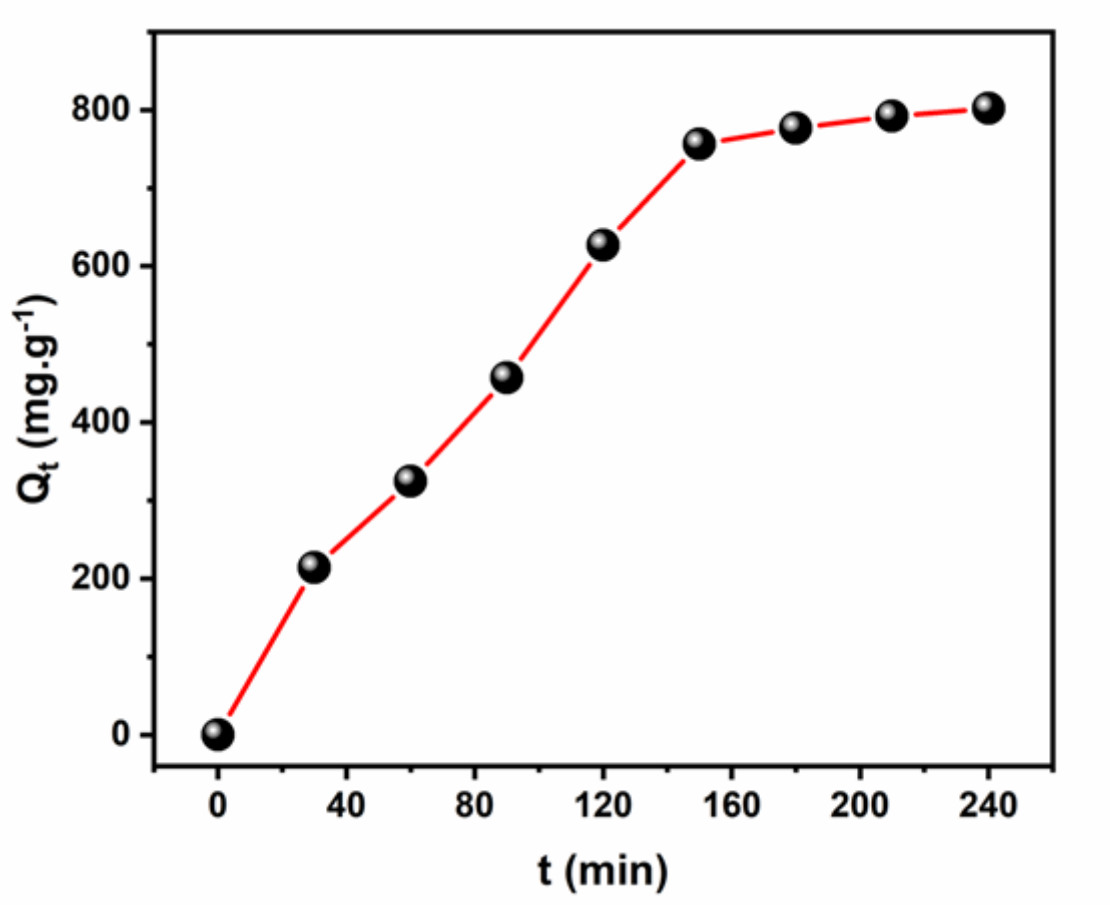

Figure 10

Effect of contact time (PCs concentration, 4000 mg L^{-1}; volume of OMWW, 25 mL; temperature, 20 °C and pH = 4.0)

Figure 11

Adsorption kinetics: pseudo-first-order (a) and pseudo-second-order (b) kinetics models of PCs derived from OMWW effluent on bio-sorbent

Figure 12

Effect pH (at 20 °C; adsorbent = 25 mg and PCs concentration, 4000 mg L^{-1})

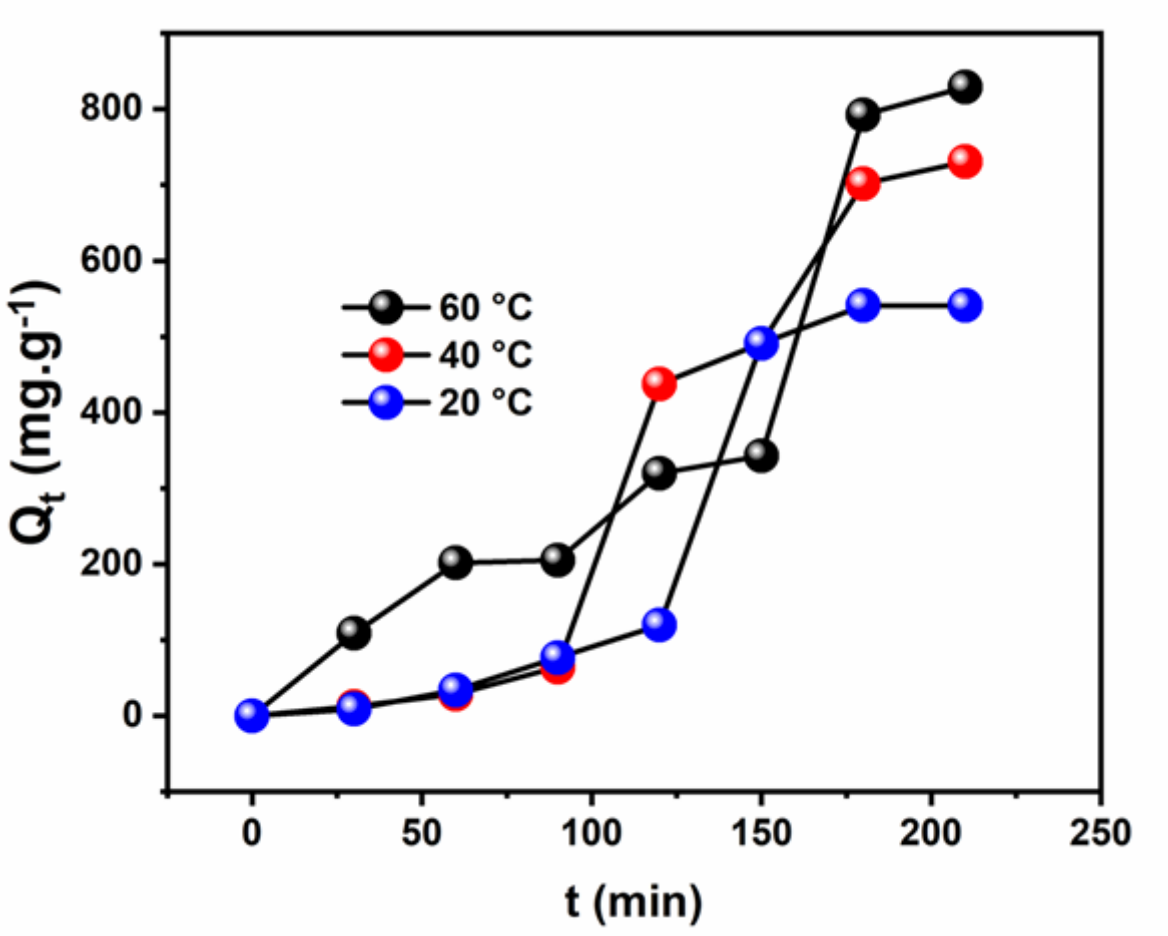

Figure 13

Effect of temperature (PCs concentration, 4000 mg L^{-1}; volume of OMWW, 5 mL; temperature, 19 °C; pH = 4.0; and contact time, 240 min)

Figure 14

$\ln(K_c)$ as function of 1/T (R^2=0.9599)

Figure 15

Predicted and experimental predicted breakthrough curves for P.C.s adsorption by the bio-sorbent (PCs concentration, 4251 mg L^{-1}; pH = 4.0; and contact time, 120)

Figure 16

Adsorption-desorption cycles for OMWW (PCs concentration 4000 mg L^{-1}, 120 min)

Supplementary Files

This is a list of supplementary files associated with this preprint. Click to download.

- GraphicalAbstract.png